

Supplementary information

Improving the interfacial properties of CZTS photocathode by Ag substitution.

Ying Fan Tay,^a Shreyash Sudhakar Hadke,^{a,b,c} Mengyuan Zhang,^a Nathan Lim,^a Sing Yang Chiam,^c and Lydia Helena Wong^{a*}

a. School of Material Science and Engineering, Nanyang Technological University, 639798, Singapore

Email: lydiawong@ntu.edu.sg

b. Energy Research Institute @ NTU (ERI@N), Research Techno Plaza, X-Frontier Block, Level 5, 637553, Singapore

Interdisciplinary Graduate School, Nanyang Technological University, 637371, Singapore

c. Interdisciplinary Graduate School, Nanyang Technological University, 637371, Singapore

c. Institute of Materials Research and Engineering, A*STAR (Agency for Science, Technology and Research), 2 Fusionopolis Way, Innovis, 138634, Singapore

	Cu	Ag	Zn	Sn	S	Ag/(Cu+Ag) (%)
CZTS	2.60	0	1.56	1	5.80	0
8% Ag	1.53	0.15	1.19	1	6.04	9.38
10% Ag	1.68	0.22	1.08	1	5.45	11.58

Table 1: Atomic ratios of ACZTS films determined by SEM-EDX by taking the average of 5 points.

	4% Ag	8%Ag
0° - 30°	13.87%	22.15%
30° - 50°	18.25%	25.33%
50° - 70°	21.59%	32.63%

Table 2: Ag/(Cu+Ag) ratios determined by angle resolved XPS for 4%Ag and 8%Ag absorbers for 3 different take-off angle channels.

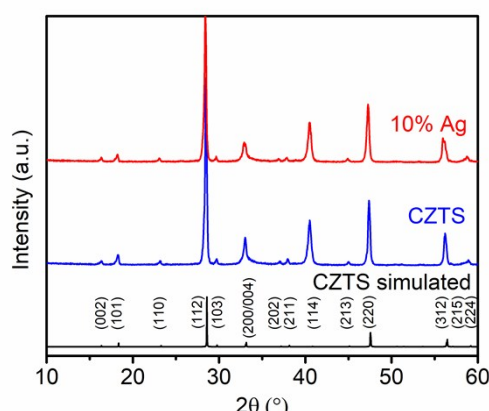


Figure S 1: X-ray diffraction spectra for CZTS and highest substituted 10%Ag thin films.

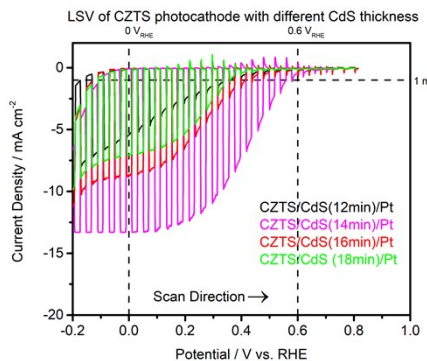


Figure S 2: Current density (J) – vs potential curves (V) of CZTS/CdS(x)/Pt in 1M K_2HPO_4/KH_2PO_4 solution (pH 7) under chopped solar -simulated AM 1.5G light illumination. X represents CdS chemical bath deposition time. 14min is determined to be the optimized CdS thickness for PEC setup.

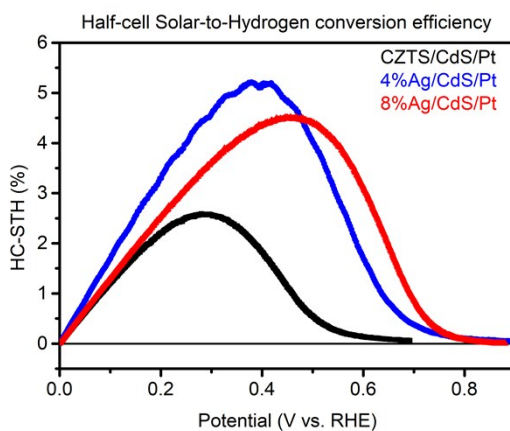


Figure S 3: HC-STH efficiency curve for $(Cu_{1-x}Ag_x)_2ZnSnS_4/CdS/Pt$ photocathodes in 1M K_2HPO_4/KH_2PO_4 solution (pH 7) under constant solar-illuminated AM 1.5G light irradiation.

Photocathode stack	Method of Onset Potential Determination			
	Potential at photocurrent of 0.05 mA cm^{-2}	Potential at photocurrent of 0.1 mA cm^{-2}	Potential where photocurrent almost disappears	Start of derivative curve
CZTS (this work)	$0.7\text{ V}_{\text{RHE}}$	$0.55\text{ V}_{\text{RHE}}$	$> 0.7\text{ V}_{\text{RHE}}$	$0.65\text{ V}_{\text{RHE}}$
8%Ag (this work)	$0.88\text{ V}_{\text{RHE}}$ (excluding photocurrent transients) $> 0.95\text{ V}_{\text{RHE}}$ including photocurrent transients	$0.72\text{ V}_{\text{RHE}}$	$> 0.9\text{ V}_{\text{RHE}}$	$0.85\text{ V}_{\text{RHE}}$
[¹] ZnSe.CIGSe/CdS/Ti/Mo/Pt	$0.89\text{ V}_{\text{RHE}}$			
[²] CIGSe/CdS/Pt			$0.75\text{ V}_{\text{RHE}}$	
[³] CIGZS/CdS/TiO ₂ /Pt			1 V_{RHE}	

[4] ACGSe/CdS/Pt	0.7 V _{RHE}			
[5] CZTS/CdS/TiO ₂ /Pt	0.86 V _{RHE}			
[6] CZTGS/CdS/In ₂ S ₃ /Pt	0.6 V _{RHE}			
[7] CBTSSe/CdS/TiO ₂ /Pt	0.56 V _{RHE}			
[8] p-InP/TiO ₂ /Pt	0.8 V _{RHE}			
[9] CIGS/CdS/Pt	0.89 V _{RHE}			
[10] Cu ₂ O/AZO/TiO ₂ /Pt		0.7 V _{RHE}		
[11] Cu ₂ O/NiMo		0.53 V _{RHE}		

Table 3: Selected photocathodes reported in literature with the different photocathode stacks, method of determining onset potential and reported onset potentials. Papers reporting onset potential without definition of how it is derived is not being listed here.

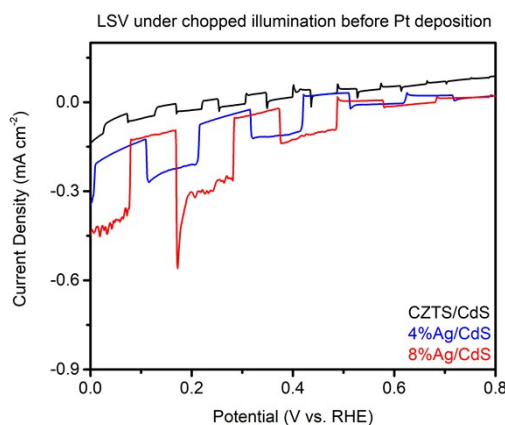


Figure S 4: Current density-potential curves of ACZTS/CdS photocathodes in Na₂SO₄ (pH 9.5) solution under chopped solar-simulated AM1.5G light irradiation before platinum catalyst deposition.

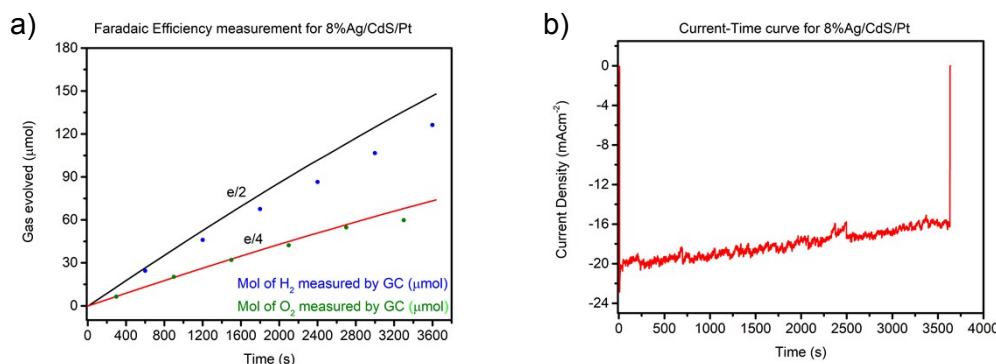


Figure S 5: (a) Time course curve for H₂ and O₂ evolution over 8%Ag/CdS/Pt in 1M K₂HPO₄/KH₂PO₄ solution (pH 7) under simulated sunlight (AM 1.5G) at 0 V_{RHE} applied potential. Solid line represents time course curve for one-half of the electrons passing for H₂ and one-quarter of the electrons for O₂. (b) Corresponding current-time curve for the Faradaic efficiency measurement.

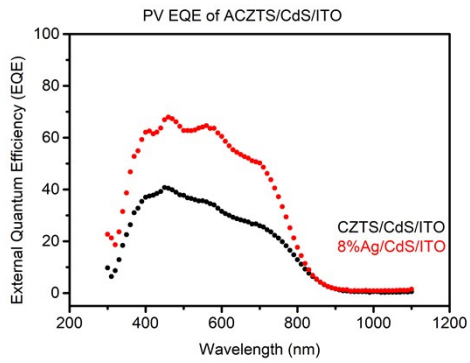


Figure S 6: PV EQE of ACZTS/CdS/ITO photovoltaic (PV) cells with CdS optimized for PEC.

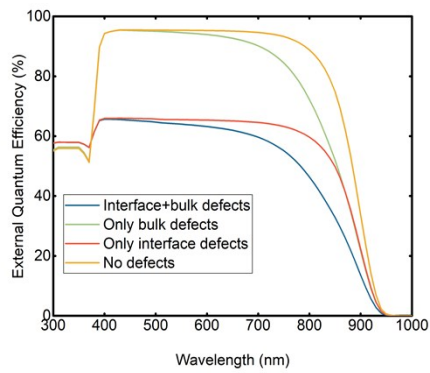


Figure S 7: Drift-diffusion simulations of CZTS/CdS with bulk and interface defects and a combination of both.

	CZTS	CdS
Bandgap (eV)	1.5	2.4
Electron affinity (eV)	4.0	4.2
Dielectric constant	6.8	10
Conduction band effective DOS (cm^{-3})	2.2×10^{18}	2.2×10^{18}
Valence band effective DOS (cm^{-3})	1.8×10^{19}	1.8×10^{19}
Electron thermal velocity (cm/s)	10^7	10^7
Hole thermal velocity (cm/s)	10^7	10^7
Electron mobility (cm^2/Vs)	100	100
Hole mobility (cm^2/Vs)	25	25
Carrier concentration (cm^{-3})	10^{15}	10^{17}
	Bulk defect	Interface defect
Type	Single acceptor	Acceptor
Electron capture cross section (cm^2)	10^{-14}	5×10^{-14}
Hole capture cross section (cm^2)	10^{-16}	10^{-14}
Energetic distribution	Gaussian, 0.25 V above VB	Gaussian, 0.6 V above VB
Total defect density	$2.3 \times 10^{15} \text{ cm}^{-3}$	$8 \times 10^{12} \text{ cm}^{-2}$

Table 4: Parameters used for SCAPS simulation in Figure S7.

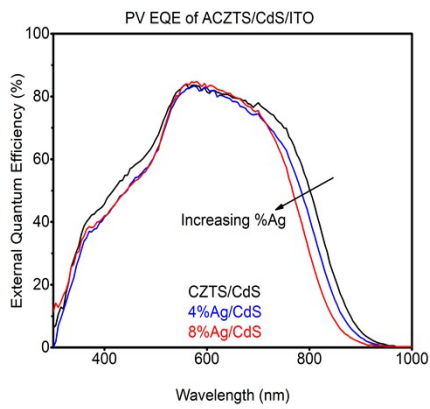


Figure S 8: PV EQE of ACZTS/CdS/ITO with CdS optimized for PV.

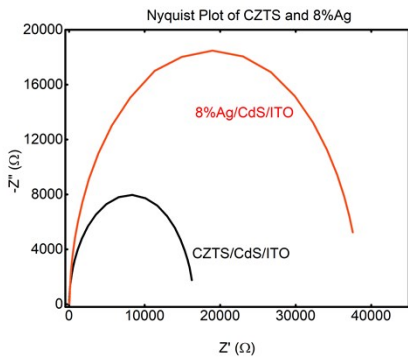


Figure S 9: Nyquist plots of CZTS/CdS/ITO and 8%Ag/CdS/ITO done in PV setup.

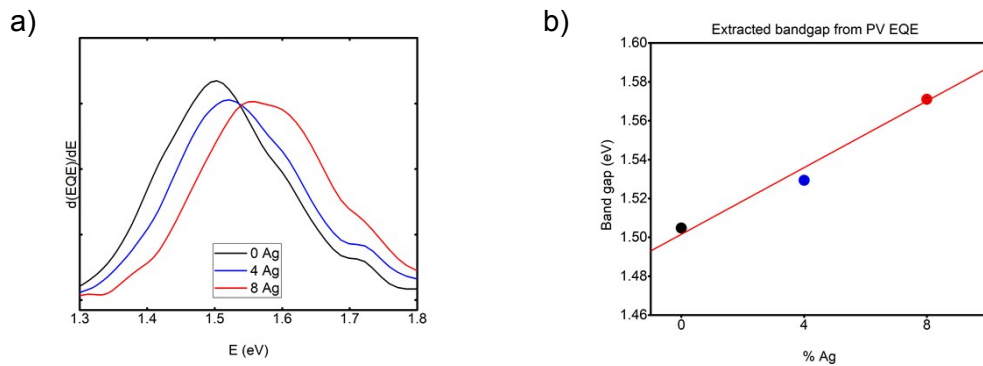


Figure S 10: (a) $d(\text{EQE})/dE$ plots of ACZTS/CdS using optimized PV CdS. (b) Corresponding extracted bandgap of ACZTS.

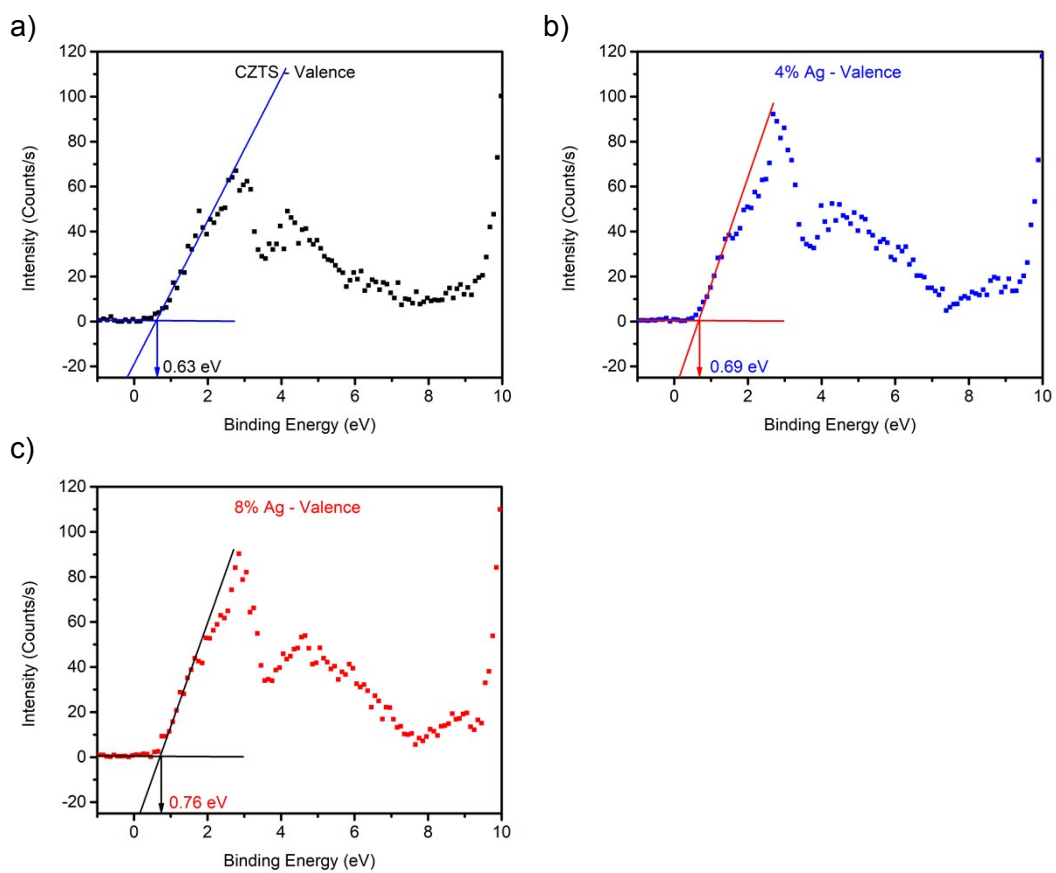


Figure S 11: Valence scans of (a) CZTS, (b) 4%Ag and (c) 8%Ag absorbers.

1. H. Kaneko, T. Minegishi, M. Nakabayashi, N. Shibata, Y. Kuang, T. Yamada and K. Domen, *Advanced Functional Materials*, 2016, **26**, 4570-4577.
2. H. Kobayashi, N. Sato, M. Orita, Y. Kuang, H. Kaneko, T. Minegishi, T. Yamada and K. Domen, *Energy & Environmental Science*, 2018, **11**, 3003-3009.
3. T. Hayashi, R. Niishiro, H. Ishihara, M. Yamaguchi, Q. Jia, Y. Kuang, T. Higashi, A. Iwase, T. Minegishi, T. Yamada, K. Domen and A. Kudo, *Sustainable Energy & Fuels*, 2018, **2**, 2016-2024.
4. L. Zhang, T. Minegishi, J. Kubota and K. Domen, *Physical chemistry chemical physics : PCCP*, 2014, **16**.
5. W. Yang, Y. Oh, J. Kim, M. J. Jeong, J. H. Park and J. Moon, *ACS Energy Letters*, 2016, **1**, 1127-1136.
6. X. Wen, W. Luo, Z. Guan, W. Huang and Z. Zou, *Nano Energy*, 2017, **41**, 18-26.
7. Y. Zhou, D. Shin, E. Ngaboyamahina, Q. Han, C. B. Parker, D. B. Mitzi and J. T. Glass, *ACS Energy Letters*, 2018, **3**, 177-183.
8. Y. Lin, R. Kapadia, J. Yang, M. Zheng, K. Chen, M. Hettick, X. Yin, C. Battaglia, I. D. Sharp, J. W. Ager and A. Javey, *The Journal of Physical Chemistry C*, 2015, **119**, 2308-2313.
9. W. Septina, Gunawan, S. Ikeda, T. Harada, M. Higashi, R. Abe and M. Matsumura, *The Journal of Physical Chemistry C*, 2015, **119**, 8576-8583.
10. T. Wang, Y. Wei, X. Chang, C. Li, A. Li, S. Liu, J. Zhang and J. Gong, *Applied Catalysis B: Environmental*, 2018, **226**, 31-37.
11. C. G. Morales-Guio, L. Liardet, M. T. Mayer, S. D. Tilley, M. Grätzel and X. Hu, *Angewandte Chemie International Edition*, 2015, **54**, 664-667.